

RSC Advances



This is an *Accepted Manuscript*, which has been through the Royal Society of Chemistry peer review process and has been accepted for publication.

Accepted Manuscripts are published online shortly after acceptance, before technical editing, formatting and proof reading. Using this free service, authors can make their results available to the community, in citable form, before we publish the edited article. This *Accepted Manuscript* will be replaced by the edited, formatted and paginated article as soon as this is available.

You can find more information about *Accepted Manuscripts* in the [Information for Authors](#).

Please note that technical editing may introduce minor changes to the text and/or graphics, which may alter content. The journal's standard [Terms & Conditions](#) and the [Ethical guidelines](#) still apply. In no event shall the Royal Society of Chemistry be held responsible for any errors or omissions in this *Accepted Manuscript* or any consequences arising from the use of any information it contains.

Fabrication and electrochemical characterization of Pt-Pd impregnated nanocomposite polymer electrolyte membranes for high concentration DMFCs

Sethu Sundar Pethaiah^{a,b,*,#}, Mani Ulaganathan^{b,#}, Ramalinga Viswanathan Mangalaraja^{c,#},

Siew Hwa Chan^{b,*},

^a *Technical University Munich - Campus for Research Excellence and Technological Enterprise, 1 CREATE Way, Singapore 138602, Singapore^c*

^b *Energy Research Institute @NTU, Nanyang Technological University, 50 Nanyang Drive, Singapore 637553, Singapore*

^c *Advanced Ceramics and Nanotechnology Laboratory, Department of Materials Engineering, University of Concepcion, Concepcion 407-0409, Chile*

Abstract

Bimetallic Pt-Pd impregnated nanocomposite polymer electrolyte membranes were prepared and the influence of Pd on Pt was evaluated towards a single cell performance. The fabricated membranes were characterised by X-Ray Diffraction (XRD) and Field-Emission Scanning Electron Microscopy (FESEM) attached with Energy Dispersive X-Ray (EDX) spectroscopy for identifying the structural and morphological characteristics, respectively. It was observed that the particle size of the bimetallic particle was increased with the increase of Pd content; the bimetallic particles were uniformly deposited with closely packed structure on the membrane surface. The performance of direct methanol fuel cells (DMFC) with normal membrane electrode assembly (MEA) and Pt-Pd impregnated nanocomposite with various compositions were studied for different methanol concentrations. Pt-Pd nanocomposite MEA with 76.91: 23.09 of atomic ratio exhibited an optimal performance with the maximum power density of 52.5 mWcm⁻². The result was benchmarked with MEA using commercially available Pt/C catalyst.

Keywords: Direct Methanol Fuel Cell, Pt-Pd bimetallic, Methanol Crossover, Fuel cell

* *Corresponding Author:* sundar.pethaiah@tum-create.edu.sg, mschan@ntu.edu.sg, Phone: +65 65923013;

Fax: +65 68969950; #Equally contributed

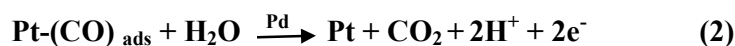
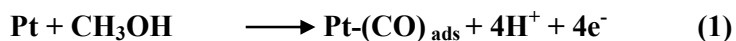
1. Introduction

The rising global energy demand and the environmental impact of energy utilization from conventional sources pose serious challenges to environmental protection and the sustainability of natural resources. Hence, in recent years there has been a significant increase in research and development activities towards renewable energy. Among the variants, fuel cells are expected to play an increasingly important role in the future because of their high fuel conversion efficiency and environmental compatibility. In particular, direct methanol fuel cell (DMFC) is a promising candidate for portable electronic devices and electric vehicles (EV) applications, because DMFC is a low-temperature energy conversion device with a simple design and virtually do not need any fuel reformer. Methanol is easily handled, stored and possibly can be derived from renewable sources. Moreover, methanol has high volumetric energy density ($4.82 \text{ kWh}\cdot\text{L}^{-1}$) compared to pressurized hydrogen ($0.18 \text{ kWh}\cdot\text{L}^{-1}$ at 1000 psi, 25°C)¹. However, some issues such as cost and durability are the major concerns of DMFC, particularly sluggish methanol oxidations and methanol crossover from anode to cathode side of DMFC. These issues might be overcome before the commercialization can take place²⁻⁵.

Membrane electrode assembly (MEA) is a key component to improve sluggish methanol oxidations and to reduce methanol crossover. As a result many research groups are working in the MEA development, though significant progress has been achieved in MEA development for DMFCs during the last decade³⁻¹⁰, yet there is a scope for research to develop a better methanol impermeable MEA with high electrode activity and stability. It is well known that Platinum(Pt) shows highest activity and stability for alcohol oxidation in acid medium, but it is easily poisoned by the CO intermediates formed in this reaction¹¹.

Moreover, cost and availability of Pt limits its usage in fuel cells. Hence, an attempt has been made to develop a multifunctional MEA to solve methanol crossover as well as sluggish methanol oxidations reaction (MOR) with a suitable catalyst.

There are number of catalyst systems including Pt-Ru, Pt-Sn, Pt-Rh, Pt-Mo, Pt-Pd, Pd-Ni and composite membrane for DMFC have been investigated^{12, 3-4}. Among them, our literature review revealed that the preparation of Pt-Pd impregnated nanocomposite polymer electrolyte membrane (PEM) by the non-equilibrium impregnation-reduction (NEIR) method is a promising method to achieve a multifunctional purpose as stated above^{13, 14}. The fabrication of Pt-Pd impregnated nano-composite PEM is a simple process making it attractive for catalyst layer preparation. The electrodes prepared by this method are few microns thickness, hydrophilic, porous and they exhibit excellent adhesion and durability³. Moreover, Pd is impermeable to methanol and its synergistic effect between Pt and Pd enhances the electrocatalytic activity towards methanol oxidation reaction⁶⁻⁸. The presence of Palladium dilutes the Pt sites and prevents the presence of three adjacent sites that are necessary for the adsorption of poison species on the electrode surface. This leads to the overall enhancement of methanol oxidations. The bifunctional mechanism of Pt-Pd nanoparticle is explained below¹⁵,



To the best of our understanding, no work has been studied on the Pt-Pd impregnated nano-composite PEMs by non-equilibrium impregnation-reduction method for DMFC applications. Hence, in this study Pt-Pd impregnated nano-composite PEMs was prepared and the effect of Pd on Pt was evaluated towards a single cell performance and compared with commercial Pt/C catalyst.

2. Experimental procedure

Proton exchange membrane (Nafion 117 DuPont) and high-purity chemicals such as Pt (NH₃)₄Cl₂ (Johnson Matthey), Pd (NH₃)₄Cl₂ (Johnson Matthey), NaBH₄ (Merck), H₂SO₄ (Merck), H₂O₂ (Merck), NaOH (Merck), carbon powder (Cabot corporation), Nafion ionomer (Dupont), 40%Pt/C (Duralyst, USA), carbon cloth (Ballard) and CH₃OH (Merck) were used in the experimental work.

2.1. Membrane pre-treatment

The Nafion membrane with 183µm in thickness was pre-treated using 5 wt. % aqueous H₂O₂ solution for 30 min at 80°C and washed repeatedly with deionized water. To convert the membrane into Na⁺ form, it was treated with 0.5 M NaCl at 80 °C for 30 min and rinsed repeatedly with deionized water. The treated membrane was dried for 12 h under vacuum at a constant temperature of 80°C. The initial weight of the treated membrane was obtained to determine the amount of Pt-Pd loading on the membrane surface¹⁰.

2.2. Preparation of Pt-Pd Composite membrane

Three different atomic ratios of the Pt-Pd (Pt:Pd of 90:10, 70:30, 50:50) impregnated nano-composite membranes were prepared by using non-equilibrium impregnation-reduction (NEIR) method^{13, 14} and denoted as A1, A2 and A3 respectively. Pt (NH₃)₄Cl₂ and Pd (NH₃)₄Cl₂ were used as Pt and Pd precursors, respectively. In NEIR method, one side of the membrane was placed to face the methanol-water (1:3) mixture of impregnation solution with appropriate Pt and Pd precursors concentrations. After the impregnation process, the reducing process follows with 10 mM of NaBH₄ at pH 13 for 2 h. The solutions were stirred in both steps at 190 rpm and 50°C. Finally, the Pt-Pd nanocomposite membranes were soaked in 0.5 M H₂SO₄ for 1 h followed by deionized water rinsing for 1 h and then dried and weighed. For comparative evaluations Pt- impregnated nanocomposite membrane also prepared¹⁰. The resulting amount of catalyst loading was 2 mg

cm⁻², the catalyst loading was controlled by impregnation time. All impregnated composite membranes were stored in highly evacuated desiccators and used as the anode of DMFC.

2.3. Preparations of membrane electrode assembly (MEA) for DMFC

The Pt-Pd nanocomposite MEA was prepared by hot pressing the Pt-Pd coated Nafion membrane between the two gas diffusion electrodes with 1 mg cm⁻² of 40% Pt/C catalyst on anode side and 3 mg cm⁻² of Pt black on cathode side at 120 °C with a pressure of 1000 psi for 5 min. Pt-Pd was deposited on one side of Nafion membrane and used as the anode of DMFC (Fig. 1). To prepare the gas diffusion electrode, the catalyst was suspended in water and ultrasonicated by adding isopropyl alcohol and 5 wt. % of Nafion ionomer. The obtained slurry was coated on the teflonised carbon cloth. Adding another layer of 40% Pt/C with Nafion ionomer helps to insure good current collection from the thin Pt-Pd catalyzed layer and provide good contact with the gas diffusion layer. It also provided some additional catalytic activity¹⁶. For comparative evaluations, a normal MEA was prepared with 3 mg cm⁻² of 40% Pt/C for anode side and 3 mg cm⁻² of Pt black for cathode side. All MEAs anode side gas diffusion electrodes were hot pressed with uniform pores (Fig. 2). To facilitate the comparative study, the total loading of electrocatalyst, hot-pressing parameters, and geometrical area of electrodes (5 cm²) were kept constant.

2.4. Structural characterizations

X-ray diffraction (XRD) patterns of Pt-Pd nanocomposite membranes were acquired at room temperature with X'pert PRO PANalytical diffractometer using Cu-k_α radiation as the source and operated at 40 kV. The sample was scanned in the 2θ ranging from 10 to 80° for 2 s in the step-scan mode. Surface morphology, cross-sectional view and the chemical composition of the Pt-Pd impregnated nanocomposite membranes were characterized using field emission scanning electron microscopy (FESEM, Horiba, EMAX) with an energy dispersive X-ray spectroscopy (EDX) analyzer (JEOL JSM-6400).

2.5. Single cell assembly and electrochemical characterizations

Single cell experiments were performed by placing Pt-Pd nanocomposite MEA between two silicone rubber gaskets with the thickness of 0.25 mm and inserted in between two serpentine grooved graphite plates with 5 cm² active area (Fig. 3). The fixture parts were clamped together using bolts and nuts by applying uniform torque to assemble the single cell (Fig. 4). Provision was made to heat the cell with temperature control. Inlet and exit ports were available for feeding the reactants and removal of products. For comparative study, single cell using MEA with commercial catalyst and Pt- impregnated nanocomposite membrane also assembled. To facilitate the comparative evaluations, all parameters are kept constant. 2 M and 6 M concentration of aqueous methanol and oxygen were supplied to the anode and cathode side of the single cell respectively. Single cell performances were tested over the range of temperature, 30-80 °C under the pressure of 2 bars at cathode side. The cell was connected to the DC electronic load bank for the polarisation studies.

3. Results and discussions

3.1. Structural characterizations

3.1.1. XRD

XRD patterns of pristine Nafion 117, Pt catalyzed, different ratios of Pt-Pd bimetallic catalyzed composite membranes and 40% Pt/C are shown in Fig. 5. The characteristic peak obtained at 16.5 and 24.8° in the XRD patterns is associated to the Nafion membrane and Vulcan XC-72 carbon support, respectively^{17, 18}. The other peaks of Pt and Pt-Pd layered Nafion membrane demonstrated the main characteristic peaks at 2θ=40°, 47° and 68° are corresponding to the (1 1 1), (2 0 0), and (2 2 0) lattice planes of face-centered cubic (fcc) structure of Pt and Pd¹⁰. However, there is no characteristic peak of metallic Pd or Pd oxide is observed, but their presence cannot be discarded because Pd may be present in Pt lattice and formed alloy or even in an amorphous form¹⁹. Similar observations were obtained for Pt-

Ru/PEM based catalyst layered systems by Naoko Fujiwara et al and Pt-Ru-Co/PEM based catalyst system by JY. Woo et al.^{3, 20}. The XRD patterns of Commercial 40 % Pt/C catalyst demonstrated the main characteristic peaks at $2\theta = 39.8, 46.5$ and 67.71° , which confirms the fcc cubic structure of Pt. From XRD measurements, the average particle size of the Pt-Pd was calculated from the broadening of the (1 1 1) diffraction peaks using Debye-Scherrer's relation. The calculated average particle size, atomic and weight ratios are given in Table 1. It was observed that the particle size is increased with the increase of Pd content, the obtained results are close in agreement with previously reported in the literatures¹⁹.

3.1.2 FESEM with EDX

Surface image of the Pt-Pd bimetallic layered Nafion 117 membrane (sample A2) is shown in Fig. 6a. Homogeneous distribution of metal nano particles on membrane surfaces was observed. However, some cracks and shrinkage were found on the surface of the Pt-Pd coated membrane. It might be due to the residual stress between the plated Pt-Pd layer and nafion polymer membrane or caused by when preparing the sample for FESEM analysis. The crack free areas of the Pt-Pd layered are very compact, which are useful to prevent methanol from crossing over to the cathode side. It was also observed that the bimetallic particles were uniformly deposited onto the membrane and the particles were closely packed with homogeneous distribution. In order to confirm the presence of bimetallic particles and the coating thickness, the study was extended to EDX and crosssectional image analyses, respectively. Fig. 6b shows a cross-section of the Pt-Pd layered Nafion membrane. The Pt-Pd/Nafion samples were cooled to 77 K and cold fractured to examine the crosssections image of the Pt-Pd impregnated membrane, by the adhesion of Pt-Pd/Nafion membrane on the carbon tape without any Au/Pt coating²¹. The thickness of the bimetallic layer is about 1 – 2 μm and there is no free gap observed between the bimetallic layer and the membrane that implies the particles are well closely attached to the membrane. EDX spectra of the sample

A2 (Fig. 6c) also confirmed the Pt and Pd particles distribution which is consistent with the cross-sectional image of the sample and with the XRD result. The obtained atomic percentage of Pt and Pd particles are given in Table 1. The precursor complexes of Pt and Pd have the same charge (2^+) and similar structure, which enhances the incorporation rates and selectivity of the incorporation of Pt and Pd complex on nafion membrane. Hence, Pt-Pd ratio in membrane possibly equal to those in the solution³. In contrast, increasing the content of platinum atomic fraction in the deposition layer is observed, this may be due to some unaccounted losses during sample preparations and transferring Pt-Pd into solution²².

3.2. Electrochemical characterizations

3.2.2. DMFC performance

The respective performances of DMFCs with normal MEA, Pt impregnated nanocomposite MEA and various compositions of Pt-Pd impregnated nanocomposite MEA fed with different methanol concentrations (2M and 6M) at 80°C are shown in Fig. 7 and 8. From Fig.7, it is observed that the performance of the DMFC increases with the increase of Pd amount in membrane up to a certain limit; this may be due to the reduced methanol crossover and increase in catalytic activity. Above the optimum level of Pd amount in membrane, there is a decrease in the performance of DMFC. This phenomenon indicates that when the Pd content increases, the amount of couples of neighbouring Pt sites become smaller with relative decrease in catalytic activity. When Pd content is too high the performance of DMFC deteriorates due to insignificant catalytic activity of pure Pd in the catalyst layer¹¹. It was noted that Pt-Pd impregnated nanocomposite MEA with 76.91: 23.09 ratio exhibited the maximum power density of 52.5 mW cm⁻², whereas, it was about 45.87 mW cm⁻² for normal MEA and 47 mW cm⁻² for Pt impregnated nanocomposite MEA at 2M methanol at 80 °C. The open circuit voltage (OCV) of sample A3 is higher than sample A2; however, sample A2 showed better performance than sample A3, this is mainly due to

accompanied effect of larger particle size and insignificant catalytic activity of Pt-Pd catalyst in sample A3. The high OCV suggested that the methanol crossover was reduced and therefore the mixed potential at the cathode possibly decreased, the reduced methanol crossover in sample A3 is probably due to larger particle size²³; however, increasing amount of Pd in sample A3 deteriorates the DMFC performance which was due to the insignificant catalytic activity of pure Pd in the catalyst layer¹¹. Hence sample A3 demonstrates higher OCV and reduced performance than other samples.

When 6M methanol was used (Fig.8), the maximum power density of Pt-Pd nanocomposite MEA was ~1.91 times higher than that of the normal MEA. It was also noted that the maximum power density of Pt-Pd impregnated nanocomposite MEA was marginally increased or remained unchanged with further increasing in methanol concentrations, while the maximum power density of normal MEA was decreased dramatically. This is mainly due to the combined effect of methanol crossover and increase in catalytic activity of Pt-Pd nanocomposite MEA, the methanol crossover not only results in a loss of fuel but also creates a mixed potential at the cathode, leading to a lower overall cell performance⁹. In addition Pt-Pd nanocomposite MEA shows better performance than Pt nanocomposite MEA, which also confirms the catalytic activity of Pd. However, Pt nanocomposite MEA demonstrates better performance than normal MEA, this behaviour could be explained by the effect of the electrode structure. The particular structure of the catalyzed membrane could result in higher catalyst utilization with respect to the normal ones, as previously suggested in the literature for different systems²⁴.

Fig. 9 shows the open circuit voltage (OCV) of normal MEA and various compositions of Pt- Pd impregnated nanocomposite MEA fed with 2M of methanol at room temperature and 80°C. As shown in Fig.9, the OCV values increased gradually with an increase in Pd content in membrane, this is due to reduced methanol crossover²⁵. The

methanol crossover through the membrane causes a significant reduction of the cathode potential due to the direct oxidation of methanol at the cathode catalyst. This side reaction leads to the larger mixed potential; as a result in a decreased value of the OCV^{26, 27}. The OCV values increases with increasing temperature, however the increasing potential difference of normal MEA is lower than Pt-Pd composite membrane, this phenomenon support the hypothesis that the Pd is impermeable to methanol and selectively transport the hydrogen ions. It is well accepted fact that Palladium is effective hydrogen storage medium and can easily form Palladium hydride²⁸. The close packed structures of metal hydrides prevents permeation of larger molecules such as methanol and water without decreasing the proton transfer rate²⁹, this synergistic effect reduces the methanol crossover and enhances the electrocatalytic activity towards methanol oxidation reaction. The mechanism of methanol crossover inhibition is generally explained below³⁰, the impregnated metal block the passage of methanol molecules and as discussed above the proton can easily pass through the metal barriers according to the following reactions,



where M represents Pt-Pd alloy.

The stability of the Pt-Pd (at % 76.91: 23.09) impregnated nanocomposite PEM i. e., sample A2 and normal MEA were studied at an intermittent discharge rate for 100 h. Fig. 9 shows the voltage vs. time characteristics of DMFC under a constant current density of 100 mAcm⁻² at 80°C. The cell voltage of sample A2 increased slowly initially with increase time and then reached a steady state value about 0.411 V at 100 mA cm⁻². During 100 h of operation, no performance degradation was observed except a mild voltage fluctuation. In contrast, a drastic voltage drop was observed for the normal MEA over the 100 h of

operation. The obtained results were well comparable with the performances of the various catalyst impregnated membranes^{3, 7, 31, 32} and the comparisons are given in Table 2.

3.3. Conclusion

Pt-Pd bimetallic catalyst was successfully deposited directly onto the polymer electrolyte membrane by NEIR method; the optimized Pt-Pd ratio was found to be in molar ratio of 76.91: 23.09. The performance of DMFC was found to increase with Pd amount on the membrane, for a quick overview Pt-Pd nanocomposite MEA with 76.91: 23.09 ratio exhibits a peak power density of 52.5 mW cm⁻² with stable voltage of 0.411V over 100 h when loaded with 100 mA cm⁻². This enhanced performance of DMFC is due to the reduced methanol crossover and improved catalytic activity of Pt-Pd impregnated nanocomposite membrane; it was also allowed the DMFC to operate at high concentration (6 M) of Methanol. Hence, it was concluded that Pt-Pd impregnated nanocomposite membranes prepared by NEIR method can also be a very good option for reducing the methanol crossover in DMFC.

Acknowledgements

One of the author R.V.Mangalaraja acknowledges FONDECYT (No. 1130916) and CONICYT-Programa de Energia (No. PASANTIA0027; ID FAST 2750), Government of Chile for the support.

References

1. H. Liu, J. Zhang, *Electrocatalysis of Direct Methanol Fuel Cells*, WILEY-VCH, 2009.
2. F. Alcaide, G. Alvarez, P.L. Cabot, H.J. Grande, O. Miguel, A. Querejeta, *Int. J. Hydrogen Energy*, 2011, 36, 4432-4439.
3. N. Fujiwara, K. Yasuda, T. Ioroi, Z. Siroma, Y. Miyazaki, *Electrochim. Acta*, 2002, 47, 4079-4084.

4. Z. Zuo, X. Zhao and A. Manthiram, *RSC Adv.*, 2013,3, 6759-6762.
5. M. M. H. Sadrabadi, E. Dashtimoghadam, F. S. Majedi, S.Wu, A. Bertsch, H. Moaddele, *RSC Adv.*, 2013, 3, 7337-7346.
6. T. Hejze, B.R. Gollas, R.K. Sauerbrey, M. Schmied, F. Hofer, J.O. Besenhard, *J Power Source*, 2005, 140, 21-27.
7. Y. J. Kim, W. C. Choi, S. I. Woo, W. H. Hong, *Electrochim. Acta*, 2004, 49, 3227-3234.
8. T. Arikian, A.M. Kannan, F. Kadirgan, *Int. J. Hydrogen Energy*, 2013, 38, 2900-2907.
9. P. Dimitrova, K.A. Friedrich, U. Stimming, *Solid State Ionics*, 2002, 150, 115-122.
10. S. S. Pethaiah, S. Gangadharan, S.H. Chan, U. Stimming, *J Power Source*, 2014, 254, 161-167.
11. F. Alcaide, G. Alvarez, P. L. Cabot, H. J. Grande, O. Miguel, A. Querejeta, *Int. J. Hydrogen Energy*, 2011, 36, 4432-4439.
12. F. Kadirgan, S. Beyhan, T. Atilan, *Int. J. Hydrogen Energy*, 2009, 34, 4312-4320.
13. R. Liu, W. H. Her, P. S. Fedkiw, *J. Electrochem. Soc.* 1992, 139, 15-23.
14. P. S. Fedkiw, Jr. Raleigh, US patent, Pat No 4959132, 1990.
15. V. Selvaraj, M. Alagar, I.Hamerton, *J Power Source*, 2006, 160, 940-948.
16. Y. Song, Y. Wei, H. Xu, M. Williams, Y. Liu, L. J. Bonville, H. R. Kunz, James M. Fenton, *J. Power Sources* 141 (2005) 250.
17. M. Ludvigsson, J. Lindgren, J. Tegenfeldt, *J. Electrochem. Soc.* 2000, 147, 1303.
18. Huang Q, Yang H, Tang Y, Lu T, Daniel LA, *Electrochem Commun*, 2006, 8, 1220-1224.
19. S. Thanasilp, M. Hunsom, *Renewable Energy*, 2011, 36, 1795-1801.
20. J. y. Woo, K. M. Lee, B. C. Jee, C. H. Ryu, C. H. Yoon, J.H. Chung, *J. Ind. Eng.*

- Chem. 2010, 16, 688-697.
21. N. Rajalakshmi, H. Ryua, K.S. Dhathathreyan, Chem. Eng. J. 102 (2004) 241
 22. E. K. Tuseeva, A. A. Mikhailova, O. A. Khazova, V. A. Grinberg, K. D. Kourtakis, RUSS ELECTROCHEM+, 2005, 41, 1316-1324.
 23. L. Brandao, J. Rodrigues, L.M. Madeira, A. Mendes, J. Hydrogen Energy, 2010, 35 11561-11567
 24. P. Millet, R. Durand, M. Pineri, J. Hydrogen Energy, 1990, 15, 245-253.
 25. S. Yousefi , M. Zohoor, Ionics, 2013, 19, 1195-1201.
 26. P.C. Lee, T. H. Han, D. O. Kim, J. H. Lee, S. J. Kang, C. H. Chung, Y. Lee, S. M. Cho, H.G. Choi, T. Kim, E. Lee, J. D. Nam, J. Membr. Sci, 2008, 322, 441-445.
 27. Y. Min. Kim, K. W. Park, J. H. Choi, I. S. Park, Y. E. Sung, Electrochem Commun, 2003, 5, 571-574.
 28. W. C. Choi, J. D. Kim, S. I. Woo, J Power Source, 2001, 96, 411-414
 29. C. Pu, Wenhua H. Kevin L. Ley, E. S. Smotkin, J. Electrochem. Soc. 1995, 142, L119-L120
 30. J. Prabhuram, T. S. Zhao, Z. X. Liang, H. Yang, and C. W. Wong, , J. Electrochem. Soc , 2005, 152, A1390-A1397
 31. W. C. Choi, J. D. Kim, S. I. Woo, J. Hydrogen Energy, 2007, 32, 903-907
 32. H. Sun, G. Sun, S. Wang, J. Liu, X. Zhao, G. Wang, H. Xu, S. Hou, Q. Xin, J. Membr. Sci, 2005, 259, 27-33

Figure captions

Figure 1. Structure of MEA

Figure 2. Gas diffusion layer with uniform holes design

Figure 3. Graphite plate with serpentine groove

Figure 4. Single cell setup

Figure 5. X-ray diffraction analysis of prepared samples

Figure 6a. FESEM image of the sample A2

Figure 6b. Cross sectional view of sample A2

Figure 6c. EDX spectrum of the sample A2

Figure 7. Comparative evaluation of DMFC with Normal and impregnated nanocomposite MEA

Figure 8. I-V curves of DMFC with 6 M methanol feed at 80°C

Figure 9. Temperature effect on OCV values of DMFC due to methanol crossover

Figure 10. Durability study of DMFC at 100 mA cm⁻², 80°C with 2M methanol

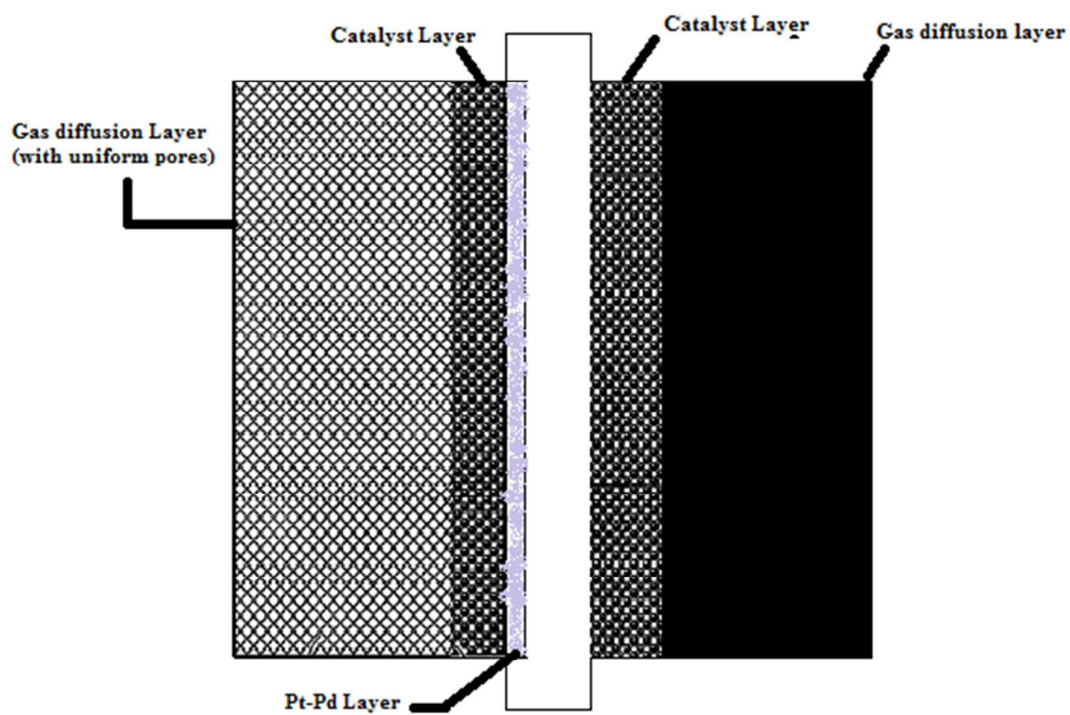


Figure 1

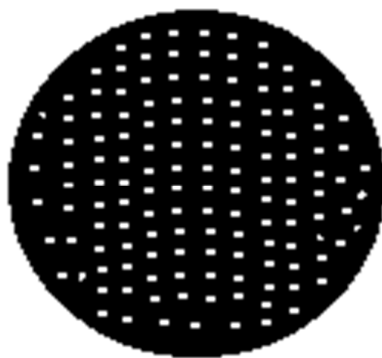


Figure 2

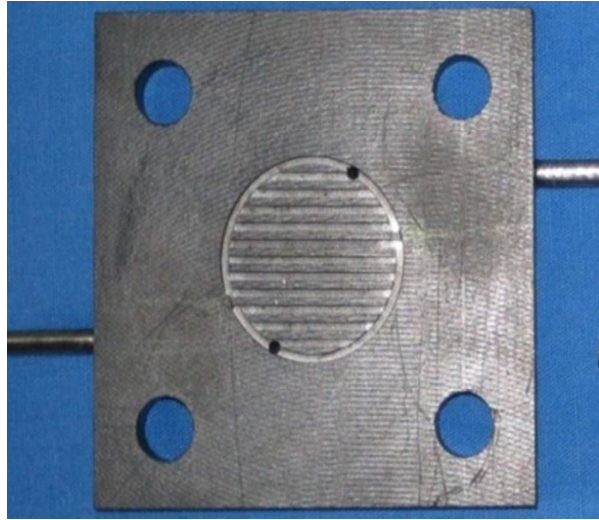


Figure 3

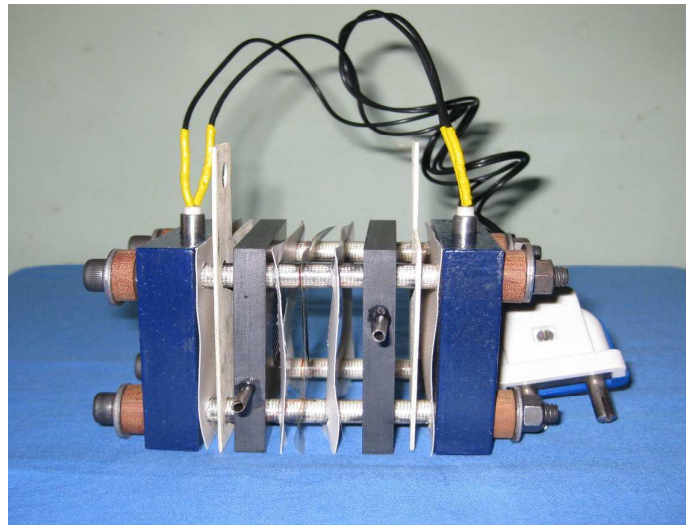


Figure 4

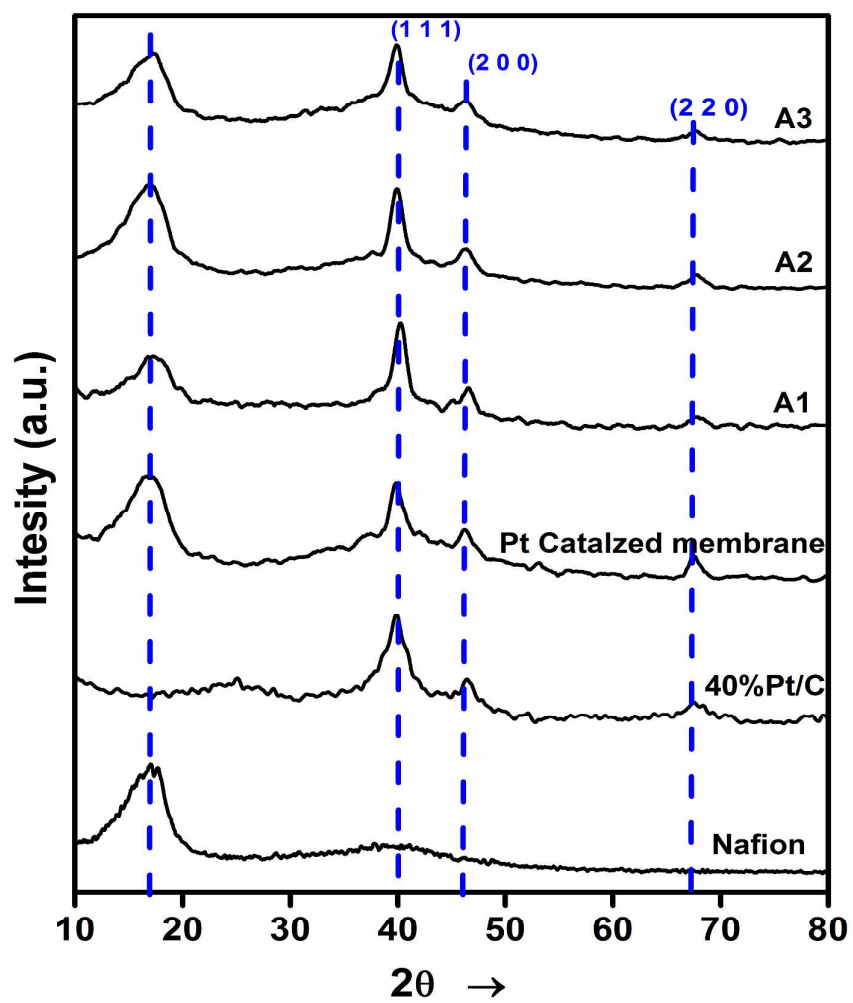


Figure 5

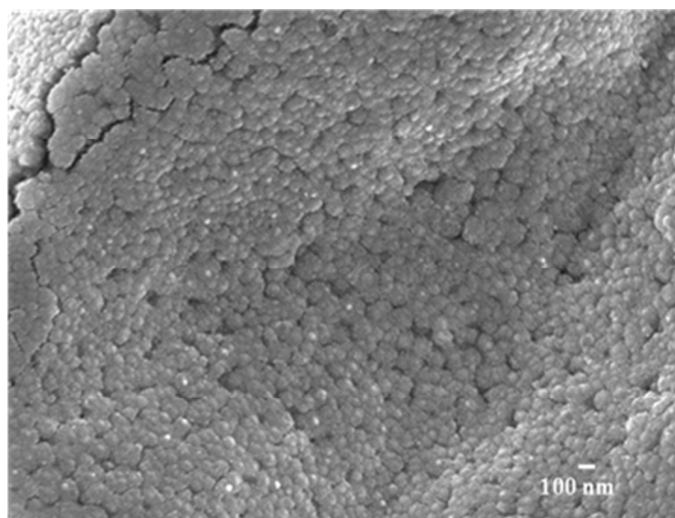


Figure 6a

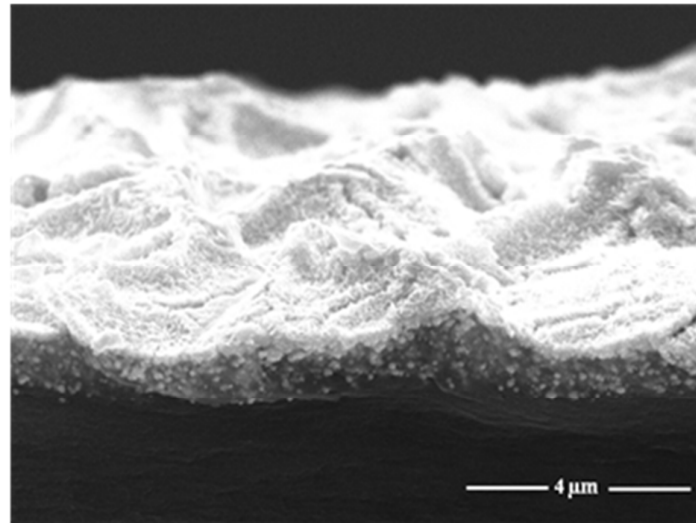


Figure 6b

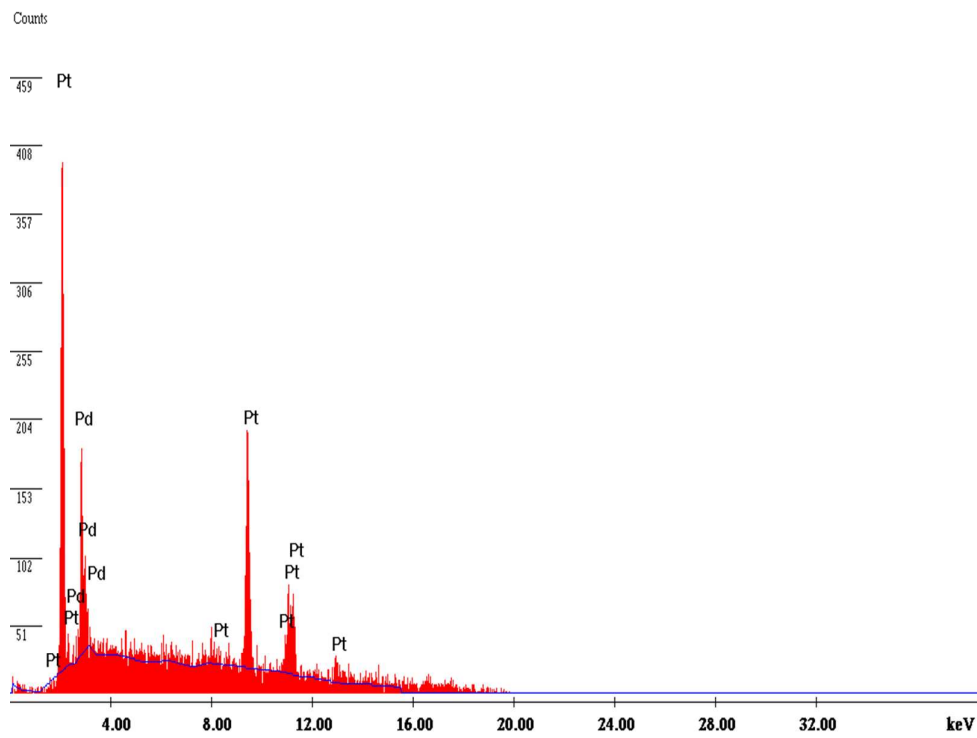


Figure 6C

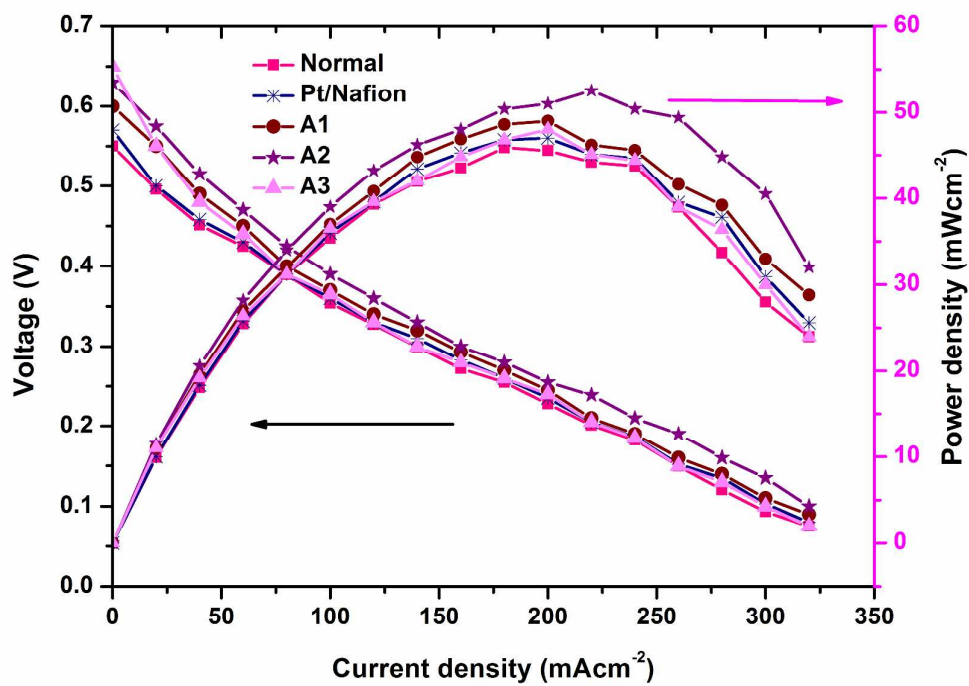


Figure 7

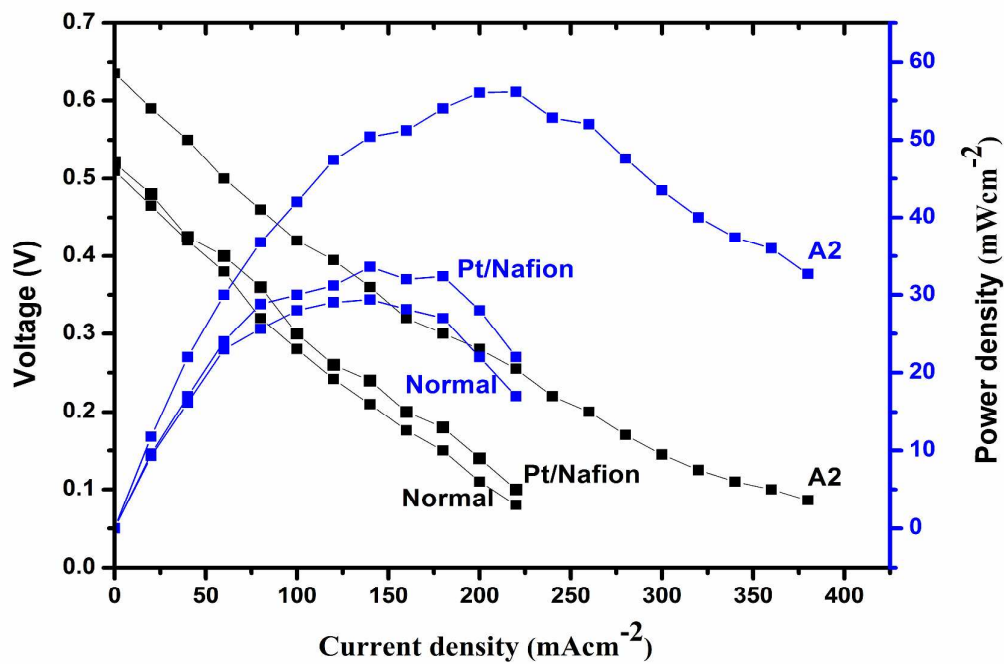


Figure 8

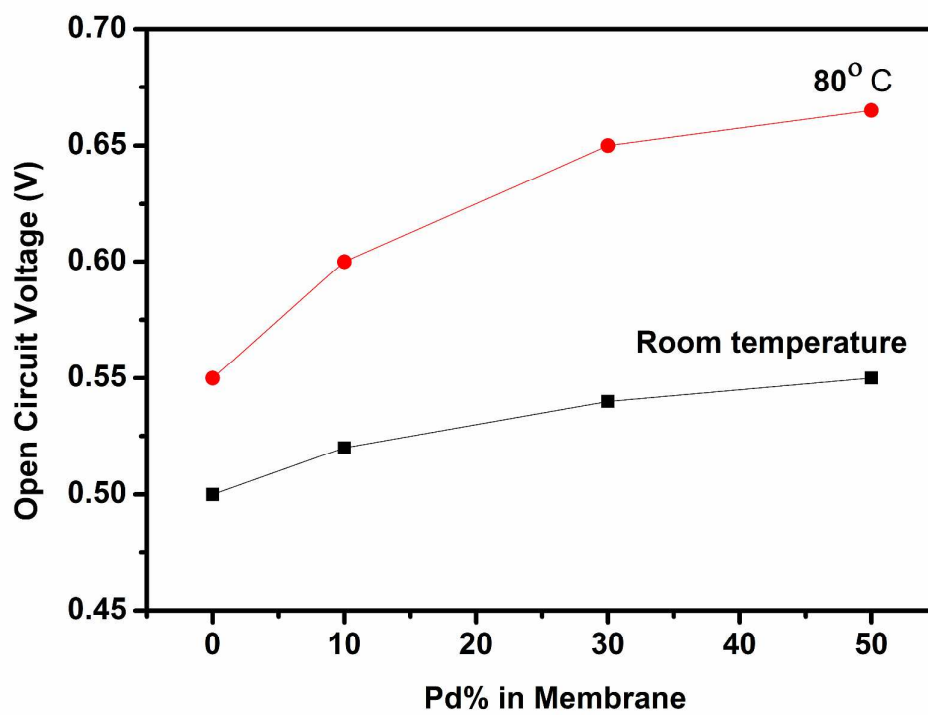


Figure 9

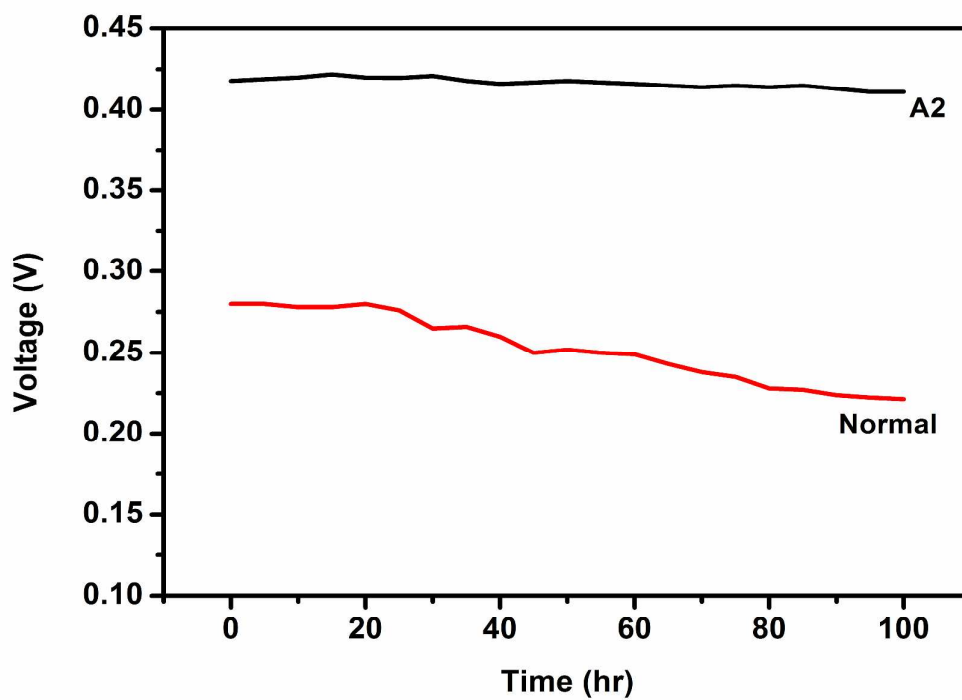


Figure 10

Table -1: XRD and EDX characteristics of the prepared samples

Sample code	Metal compositions in solution (at. %)	XRD	EDX	
		Average particle size (nm)	Metal compositions (at. %)	Metal compositions (wt. %)
A1	Pt-Pd (90:10)	5.4	94.61 : 5.39	96.98 : 3.02
A2	Pt-Pd (70:30)	5.7	76.91 : 23.09	85.93 : 14.07
A3	Pt-Pd (50:50)	6.7	62.55 : 37.45	75.39 : 24.61

Table -2: Impregnated Membrane Performance comparison from literature

Impregnated Membrane	Operating temperature/Methanol concentration	Current Density @ 0.3V(mA/cm ²)	References
Pt-Ru/Nafion	120°C/1M	~ 450	3
Pt-Ru/Nafion	30°C/2M	~270	31
Pd/Nafion	30°C/1M	~140	32
Pd/Nafion	40°C/2M	~130	7
Pt-Pd/Nafion	80°C/2M	160	From our study